Eur. Phys. J. C (2022) 82:739
https://doi.org/10.1140/epjc/s10052-022-10678-2

THE EUROPEAN PHYSICAL JOURNAL C

Regular Article - Theoretical Physics

Dynamics of evolving cavity in cluster of stars

Rubab Manzoor[1,a], **Saadia Mumtaz**[2,b], **Daoud Intizar**[1,c]

[1] Department of Mathematics, University of Management and Technology, Johar Town Campus, Lahore 54782, Pakistan
[2] Institute of Chemical Engineering and Technology, University of the Punjab, Quaid-e-Azam Campus, Lahore 54590, Pakistan

Received: 20 October 2021 / Accepted: 3 August 2022 / Published online: 23 August 2022

Abstract We examine the evolution of cavities within spherically symmetric cluster of stars in high curvature gravity. For this purpose, we use $f(R)$ gravity through the Starobinsky model to incorporate dark matter effects in the discussion. In particular, we check the physical significance of the $f(R)$ model by associating it with the observational data of stellar object $4U\,182030$. For evolution of the cavity, we consider the purely areal evolutionary phase by assuming that the proper distance (in a radial direction) among neighboring stars remains constant. The analytical solutions are obtained among which a few solutions fulfill the Darmois conditions. It is found that the evolution of the cavity in a cluster of stars is highly controlled by the influence of dark matter.

1 Introduction

In modern cosmology, dark matter and dark energy have been the most fascinating objectives. Planck's collaborators provided observational data that indicates 5% seen matter, 71% dark energy (DE) and 27% dark matter (DM)[1]. Dark energy is a mysterious form of energy whose presence helps to compress the curvature of space which in turn speeds up the cosmic expansion. Baryonic matter refers to the visible matter in the universe while DM is an invisible hypothetical type of matter which does not interact with electromagnetic radiations. It can only be observed via its gravitational effects on the observable matter.

The theory of $f(R)$ gravity, being an alternative candidate of general relativity (GR), has received a lot of attention due to its simplicity in describing the interaction of DE and DM [2–8]. This theory is derived by modifying the Ricci scalar in the Einstein Hilbert action to its generic function $f(R)$ that represents the higher order curvature principle for a gravitational framework. Many researchers used different models of $f(R)$ functions to describe the impact of DM and DE [9–13]. In this context, Starobinsky [14,15] used the second order curvature term, $f(R) = R + \epsilon R^2$, to formulate Einstein's equations with a quantum one loop system. He used this model to describe the exponential cosmic expansion and current time cosmic acceleration for an early time as well as the present time of power-law inflation. This model can also deal with DM issues [16].

Until about a decade ago, star clusters in general, and globular clusters in specific were assumed to be basic formations composed of gravitationally bound stars with a common origin [17]. Many observational surveys like the rotational loops (out to tens of kpc), gravitational lensing (out to 200 kpc), and heat in clusters showed that 95% of a cluster of stars is made up of any unknown segment of DM [18–20]. The challenges of galactic rotational curves, stellar clusters and mass differences lead to the presence of DM in cluster evolution [21–23]. Thus it exhibits influence of DM in the evolutionary mechanism. This may enable us to unveil some hidden facts that are not yet detectable in the universe's structure. In this context, many useful theoretical works have been done to explore the evolution and development of stellar structures [24–29].

At the large scale, about 80% of the universe volume is composed of cosmic voids. These voids are large spaces between clusters of stars, which contain very few or no stellar structures. Cosmic voids are not empty, but they are underdense enough that the phenomenon of gas-stripping galaxies is extremely rare. In this way, these voids provide a unique environment for the description of the evolution and formation of galaxies [30]. It is believed that the actual universe has a sponge-like structure governed by the voids [31]. Many observations indicate that voids of a characteristic scale of 30 h^{-1} Mpc exist in the present volume of the universe, where h shows the dimensionless Hubble parameter, $H_0 = 100$ h km s^{-1}Mpc^{-1} [32]. However, voids of different sizes, rang-

[a] e-mails: rubab.manzoor@umt.edu.pk; dr.rubab.second@gmail.com
[b] e-mail: saadia.icet@pu.edu.pk (corresponding author)
[c] e-mail: daoudchoudhary1673@gmail.com

ing from minivoids [33] to supervoids [34] can be discovered. According to Λ cold DM (Λ CDM) simulations, voids should have a density of low-mass halos of about 1/10 the cosmic mean. Many researchers also noticed that the galaxies have a poor tendency to get higher rates of star formation towards void centers. It is important to notice that voids are neither spherical nor empty in general. In simulation results or deep redshift observations, voids are generally referred to spherical vacuum cavities surrounded by a fluid.

The issue of cavity evolution followed by a central explosion of a spherically symmetric distribution was firstly discussed by Skripkin [35]. Accordingly, a cavity appears around the center of fluid distribution under a constraint called the Skripkin condition. This topic has been studied in detail, demonstrating that the scalar expansion disappears under the Skripkin conditions (for isotropic fluid with the constant distribution of energy density). A further detailed study on this problem declared that expansion less fluid distribution requires the existence of a cavity within the system [36]. Herrara et al. [37] studied the evolution of expansion-free isotropic fluid and found that the Skripkin model is not consistent with the Darmois junction conditions [38]. Also, expansion-free homogeneous dust fluid fails to attain physical interest because of negative energy density. Herrera et al. [39] also discussed the evolution of the cavity by using the constant proper radial distance between fluid neighboring particles. Sharif and Bhatti [41] described shear-free cavity models with plane symmetry. Yousaf and Bhatti [42] discussed the cavity evolution and instability of relativistic systems. Sharif and Mumtaz [43–45] studied the dynamics of collapsing gaseous masses with and without dissipative effects.

In this paper, we discuss evolution of the cavity for a spherically symmetric cluster of stars in the context of $f(R)$ gravity. For this purpose, we consider purely areal evolution in which variation of the proper radial distance between any two infinitesimally small particles of fluid per unit of proper time vanishes [39]. We are particularly interested in analytical models that, despite being relatively simple to assess, incorporate some of the key characteristics of an actual situation. It should be noted that we are only interested in the evolution of cavity, not in the dynamics and conditions of its formation. In this context, the fluid is constrained by two hypersurfaces. The external hypersurface separates the fluid distribution from a Schwarzchild or Vaidya spacetime (depending on whether we assume the evolution to be adiabatic or dissipative) and the internal one is taken as Minkowski spacetime that delimits the cavity.

In general, voids are neither spherical nor empty but for simplicity, we can model vacuum spherical cavities within the cluster of stars as a predecessor of voids. The paper is formatted as follows. Section 2 describes general formalism of $f(R)$ theory. The next section deals with a spherically symmetric cluster of stars in the $f(R)$ model along with junction conditions. In Sect. 4, we apply the Strobinsky model whereas Sect. 5 deals with the purely areal evolution as compared to the radial velocity and describes different models of the cavity in a cluster of stars. Section 6 summarizes our results.

2 The $f(R)$ theory

The $f(R)$ theory is followed by the action [2–8]

$$S_f(R) = \frac{1}{\kappa}\int d^4x\sqrt{-g}\,f(R) + S_M. \tag{1}$$

Here κ shows the coupling constant, S_M represents the matter related segment and $f(R)$ describes a non-linear Ricci scalar part. The metric $f(R)$ field equations are obtained by varying (1) with respect to $g_{\iota\omega}$ as follows

$$R_{\iota\omega}f(R) - \frac{1}{2}f(R)g_{\iota\omega} + (g_{\iota\omega}\Box - \nabla_\iota\nabla_\omega)f_R = \omega T_{\iota\omega}, \tag{2}$$

where $R_{\iota\omega}$ represents Ricci tensor, $f_R = \frac{df}{dR}$, and $T_{\iota\omega}$ shows ideal energy momentum tensor for matter distribution given by

$$T_{\iota\omega} = -\frac{2}{\sqrt{-g}}\frac{\delta S_M}{\delta g^{\iota\omega}}. \tag{3}$$

Equation (2), in terms of Einstein tensor, can be composed as

$$G_{\iota\omega} = \frac{\kappa}{f_R}[(T_{\iota\omega} + T^{(D)}_{\iota\omega})], \tag{4}$$

with

$$T^{(D)}_{\iota\omega} = \frac{1}{\kappa}\nabla_\iota\nabla_\omega f_R - \Box f_R g_{\iota\omega} + (f - Rf_R)\frac{g_{\iota\omega}}{2}, \tag{5}$$

where the superscript D represents dark source parts (may be DE or DM).

3 Model of cluster of stars

To discuss cavity formation in the cluster of stars, we consider a cluster that is composed of compact stars and exotic material like DM. These types of clusters are found in some dwarf irregular galaxies [40]. Since clustering of stars involves a strong gravitational field thus we model the cluster of stars as a system of self-gravitating fluid having DM and stars as fluid particles. Specifically, we assume a spherically symmetric distribution of star cluster, circumscribed by a spherical surface. The system is considered to be locally anisotropic, experiencing dissipation as a heat flow in diffusion approximation. The general interior metric (in comoving coordi-

nates) is given as

$$ds^2 = -A^2dt^2 + B^2dr^2 + C^2(d\theta^2 + \sin^2 d\phi^2), \tag{6}$$

where A, B and C are positive functions of t and r. We take the coordinates $x^0 = t$, $x^1 = r$, $x^2 = \theta$, $x^3 = \phi$. The coordinates C and r have the same dimensions whereas A and B are dimensionless. According to Eq. (6), the term $\int Bdr$ denotes proper radius inside any spherical hypersurface $\Sigma^{(e)}$ and C is the areal radius. The energy-momentum distribution inside $\Sigma^{(e)}$ is given by

$$T_{\iota\omega}^{(-eff)} = \left(\mu^{eff} + P_{\perp}^{eff}\right)V_\iota V_\omega + P_{\perp}^{eff} g_{\iota\omega} + \left(P_r^{eff} - P_{\perp}^{eff}\right)\chi_\iota\chi_\omega + q_\iota^{eff} V_\omega + V_\iota q_\omega^{eff}. \tag{7}$$

Here μ^{eff}, p_r^{eff}, q_ι^{eff}, V^ι and χ^ι represent energy density, radial pressure, dissipation term describing heat flux, four velocity and radial unit four-vector, respectively. The four vectors satisfy the following identities

$$V^\iota V_\iota = -1, \quad V^\iota q_\iota = 0, \quad \chi^\iota\chi_\iota = 1, \quad \chi^\iota V_\iota = 0. \tag{8}$$

Moreover

$$\mu^{eff} = (\mu^D + \mu), \tag{9}$$
$$q^{eff} = (q^D + q), \tag{10}$$
$$P_r^{eff} = (P_r^D + P_r), \tag{11}$$
$$P_{\perp}^{eff} = (P_{\perp}^D + P_{\perp}), \tag{12}$$

where superscript D represent DM contributions and the terms without superscript indicate baryonic matter terms.

The $f(R)$ field equations for the line element (6) are given by

$$G_{00} = \mu^{eff} = \frac{\kappa}{f_R}(T_{00} + T_{00}^D) = \frac{A^2R}{2} - \frac{1}{f(R)}\left(f_{R;r;r} - B\dot{B}\dot{f}_R - \frac{B'}{B}f'_R - \kappa A^2\mu + \frac{A^2 f}{2}\right), \tag{13}$$

$$G_{11} = P_r^{eff} = \frac{\kappa}{f_R}(T_{11} + T_{11}^D) = \left(\frac{B^2 f}{2} - f_{R;r;r} + \frac{B\dot{B}}{A^2}\dot{f}_R + \frac{B'}{B}f'_R + \kappa B^2 P_r\right)\frac{1}{f(R)} - \frac{B^2R}{2}, \tag{14}$$

$$G_{22} = P_{\perp}^{eff} = \frac{\kappa}{f_R}(T_{22} + T_{22}^D) = \left(\frac{R^2 f}{2} - f_{R;\theta;\theta} - \frac{R\dot{R}}{A^2}\dot{f}_R + \frac{RR'}{B^2}f'_R + \kappa R^2 P_{\perp}\right)\frac{1}{f(R)} - \frac{R^3}{2}, \tag{15}$$

$$G_{01} = q^{eff} = \frac{\kappa}{f_R}(T_{01} + T_{01}^D) = -\frac{1}{f(R)}\left(f_{R;t;0} - \frac{2A'}{A}\dot{f}_R - \frac{\dot{B}}{B}f'_R + \kappa ABq\right). \tag{16}$$

The prime and dot denote differentiation with respect to r and t, respectively. The kinematics of an evolving cluster can be described with the help of four acceleration (a_α), expansion scalar (θ) and shear tensor ($\sigma_{\iota\omega}$) given by

$$a_\iota = V_{\iota;\omega}V^\omega, \quad \theta = V^\iota_{;\iota}, \tag{17}$$

$$\sigma_{\iota\omega} = V_{(\iota;\omega)} + a_{(\iota}V_{\omega)} - \frac{1}{3}\theta h_{\iota\omega}, \tag{18}$$

where

$$h_{\iota\omega} = g_{\iota\omega} + V_\iota V_\omega \tag{19}$$

represents the projection tensor. For the metric (6), we have

$$V^\iota = A^{-1}\delta^\iota_0, \quad q^\iota = qB^{-1}\delta^\iota_1, \quad \chi^\iota = B^{-1}\delta^\iota_1. \tag{20}$$

From Eqs. (17) and (20), the only non-zero four acceleration component and its scalar are written as

$$a_1 = A'A^{-1}, \quad a = (a^\iota a_\iota)^{\frac{1}{2}} = A'(AB)^{-1}, \tag{21}$$

also the expansion scalar is

$$\theta = \frac{1}{A}\left(\frac{2\left(\frac{\dot{C}}{C}\right) + \dot{B}}{B}\right). \tag{22}$$

The non-zero components of shear tensor yield

$$\sigma_{11} = \frac{2}{3}B^2\sigma, \quad \sigma_{22} = \sigma_{33}\sin^{-2}\theta = -\frac{1}{3}R^2\sigma, \tag{23}$$

and its scalar is given by

$$\sigma^{\iota\omega}\sigma_{\iota\omega} = \frac{2}{3}\sigma^2, \tag{24}$$

where

$$\sigma = \frac{1}{A}\left(\frac{\dot{B}}{B} - \frac{\dot{C}}{C}\right). \tag{25}$$

The shear tensor can also be written in terms of projection tensor as

$$\sigma_{\iota\omega} = \sigma\left(\chi_\iota\chi_\omega - \frac{1}{3}h_{\iota\omega}\right). \tag{26}$$

For the sake of convenience [46,47], the energy momentum tensor (7) can be rewritten in the following form

$$T_{\iota\omega}^{-(eff)} = \mu^{eff}V_\iota V_\omega + \hat{P}^{eff}h_{\iota\omega} + \Pi_{\iota\omega}^{eff} + q^{eff}(V_\iota\chi_\omega + \chi_\iota V_\omega), \tag{27}$$

with

$$\hat{P}^{eff} = \frac{1}{3}h_{\iota\omega}T^{(eff)\iota\omega} = \frac{P_r^{eff} + 2P_{\perp}^{eff}}{3}, \tag{28}$$

$$\Pi^{(eff)\iota\omega} = \left(h_{\gamma}^{(\iota}h_{\delta}^{\omega)} - \frac{1}{3}h^{\iota\omega}h_{\gamma\delta}\right)T^{(eff)\gamma\delta}$$
$$= \Pi^{(eff)}\left(\chi^{\iota}\chi^{\omega} - \frac{1}{3}h^{\iota\omega}\right), \tag{29}$$
$$\Pi^{(eff)} = P_r^{eff} - P_{\perp}^{eff}. \tag{30}$$

Misner and Sharp [48] introduced a mass function $m(t,r)$ which represents energy within a system [49] given by

$$m = \frac{C^3}{2}R_{23}^{23} = \frac{C}{2}\left[\left(\frac{\dot{C}}{A}\right)^2 - \left(\frac{C'}{B}\right)^2 + 1\right]. \tag{31}$$

In order to discuss the dynamical characteristics of the system, we use the proper time and radial derivatives given by [48].

$$D_T = \frac{1}{A}\frac{\partial}{\partial t}, \tag{32}$$
$$D_C = \frac{1}{C'}\frac{\partial}{\partial r}. \tag{33}$$

Using Eq. (32), we may define the velocity U of a collapsing or expanding fluid distribution as the differential of areal radius w.r.t the proper time given as

$$U = D_T C < 0, \quad U = D_T C > 0, \tag{34}$$

Equation (31), through the above equation, can be expressed as

$$E = C'B^{-1} = \left(1 - \frac{2m}{C} + U^2\right)^{\frac{1}{2}}. \tag{35}$$

Moreover, Eq. (31) along with the field equations (32) and (34) gives [36]

$$m' = 4\Pi\left(\mu^{eff} + q^{eff}\frac{U}{E}\right)C'C^2, \tag{36}$$

whose integration yields

$$m = 4\Pi\int_0^r\left(\mu^{eff} + q^{eff}\frac{U}{E}\right)C^2C'dr. \tag{37}$$

Here we consider a regular center for the system and hence $m(0) = 0$. Using Eqs. (16), (22) and (25), we get

$$q^{eff}B = \frac{1}{3}(\theta - \sigma') - \frac{\sigma C'}{C}, \tag{38}$$

which can be rewritten with the help of Eq. (33) as

$$q^{eff} = E\left(\frac{1}{3}D_C(\theta - \sigma) - \frac{\sigma}{C}\right). \tag{39}$$

The Weyl tensor describes the effects of tidal forces due to gravitational effects within the system. It is denoted by $C_{\alpha\mu\beta\nu}$ and evaluated in terms of Riemann tensor $R^{\rho}_{\alpha\beta\sigma}$, Ricci tensor R^{ρ}_{β} and Ricci scalar R as

$$C^{\rho}_{\alpha\beta\sigma} = R^{\rho}_{\alpha\beta\sigma} - \frac{1}{2}R^{\rho}_{\beta}g_{\alpha\sigma} + \frac{1}{2}R_{\alpha\beta}\delta^{\rho}_{\sigma}$$
$$-\frac{1}{2}R_{\alpha\sigma}\delta^{\rho}_{\beta} + \frac{1}{2}R^{\rho}_{\sigma}g_{\alpha\beta} + \frac{1}{6}R(\delta^{\rho}_{\beta}g_{\alpha\sigma} - g_{\alpha\beta}\delta^{\rho}_{\sigma}). \tag{40}$$

The Weyl tensor can further be converted into the electric $E_{\alpha\beta}$ and magnetic parts $H_{\alpha\beta}$. For spherically symmetric distribution, the magnetic part vanishes whereas the electric part is defined as

$$E_{\iota\omega} = C_{\iota\mu\omega\nu}V^{\mu}V^{\nu}, \tag{41}$$

or it can be written in terms of four vectors as

$$E_{\iota\omega} = \epsilon\left(\chi_{\iota}\chi_{\omega} - \frac{1}{3}h_{\iota\omega}\right). \tag{42}$$

Here

$$\varepsilon = \frac{1}{2A^2}[\ddot{C}C^{-1} - \ddot{B}B^{-1} - (\dot{C}C^{-1} - \dot{B}B^{-1})$$
$$\times(\dot{A}A^{-1} - \dot{C}C^{-1})]12B^2[A''A^{-1} - C''C^{-1}$$
$$+(B'B^{-1} + C'C^{-1})(C'C^{-1} - A'A^{-1})] - \frac{1}{2C^2}. \tag{43}$$

This equation, through the field equations and Eq. (31), can be written in terms of mass function as [36]

$$\varepsilon = 4\pi(\mu^{eff} - P_r^{eff} + P_{\perp}^{eff}) - \frac{3m}{R^3}. \tag{44}$$

3.1 Junction conditions

We assume Vaidya spacetime as an exterior spacetime (i.e., we consider massless outgoing radiation case) defined by

$$ds^2 = -\left[1 - \frac{2M(\upsilon)}{r}\right]d\upsilon^2 - 2drd\upsilon$$
$$+r^2(d\theta^2 + sin^2\theta d\phi^2), \tag{45}$$

where $M(\upsilon)$ and υ denote the total mass and retarded time, respectively. In the absence of thin shell geometry, Darmois junction conditions are used for the the matching of Vaidya spacetime to the non-adiabatic sphere, along the surface $r = constant = r_{\Sigma^{(e)}}$. These junction conditions include consistency of the $1st$ and $2nd$ fundamental forms, based on matching hypersurfaces [38]. The results of Darmois conditions yield

$$m(t,r)\overset{\Sigma^{(e)}}{=}M(\upsilon), \tag{46}$$
$$2\left(\frac{\dot{C}'}{C} - \frac{\dot{B}}{B}\frac{\dot{C}}{C} - \frac{\dot{C}}{C}\frac{A'}{A}\right)$$
$$= -\frac{B}{A}\left[2\frac{\ddot{C}}{C} - \left(2\frac{\dot{A}}{A} - \frac{\dot{C}}{C}\right)\frac{\dot{C}}{C}\right]$$
$$+\frac{A}{B}\left[\left(2\frac{A'}{A} + \frac{\dot{C}}{C}\right)\frac{C'}{C} - \left(\frac{B}{C}\right)^2\right], \tag{47}$$

and

$$q^{eff}\overset{\Sigma^{(e)}}{=}\frac{L}{4\pi^{eff}r}. \tag{48}$$

Here L represents the total luminosity of cluster given by

$$L = \left(1 - \frac{2m}{r} + 2\frac{dr}{d\upsilon}\right)^{-1} L_\infty, \tag{49}$$

with

$$L_\infty = \frac{dm}{d\upsilon}, \tag{50}$$

as the entire luminosity determined by an observer in the state of rest at infinity. Equation (47) along with the field equations provides

$$q^{eff} \overset{\Sigma^{(e)}}{=} p_r^{eff}. \tag{51}$$

In the case of cavity formation, we also apply matching conditions between the solution and the Minkowsky spacetime to delimit this cavity on the boundary surface. If $\Sigma^{(i)}$ denotes the boundary surface between the cluster fluid and the cavity, then matching conditions associated with Minkowski spacetime within the cavity and the cluster distribution give

$$m(t,r) \overset{\Sigma^{(i)}}{=} 0, \tag{52}$$

$$q^{eff} \overset{\Sigma^{(e)}}{=} P_r^{eff}. \tag{53}$$

Let us consider an empty cavity, then we have $L \overset{\Sigma^{(i)}}{=} 0$, which gives

$$q^{eff} \overset{\Sigma^{(e)}}{=} p_r^{eff} \overset{\Sigma^{(e)}}{=} 0. \tag{54}$$

4 The Starobinsky model

The $f(R)$ theory of gravity is consistent with DM and DE at a large scale (stellar object scales like clusters). Starobinsky generalized Einstein Hilbert's action with higher order curvature term to construct field equations related to quantum one loop distribution. This derived model can describe cosmic exponential expansion as well as current time cosmic acceleration for both early and current times of power-law inflation. It is defined as

$$f(R) = R + \varepsilon R^2, \tag{55}$$

with ε as a positive real number. It can solve various issues like inflation, cosmic acceleration and DE [14,15]. Moreover, it has been shown that the respective model can be used for DM problems according to WMAP data for $\varepsilon = \frac{1}{6M^2}$ with $M = 2.7 \times 10^{-12}\ GeV$, $(\varepsilon = 2.3 \times 10^{22} Ge/V^2)$. The square-order curvature term behaves like an extra degree of freedom (scalar graviton) whose interaction with standard model particles yields an abundance of the thermal energy which provides DM regions. The scalar graviton of mass $M < 10^{-12}$ generates Yukawa force of attraction between DM particles having dissimilar masses [16]. For $f(R) \to R$, GR solutions are recovered. The field equations (13)–(16) for this model become

$$G_{00} = \mu^{eff} = \frac{1}{1+2\epsilon R}\left[\mu A^2\kappa + A^2\left(\frac{-\epsilon R^2}{2}\right) - \frac{2\epsilon A^2 R''}{B^2} + \left(\frac{2\dot{C}}{C} - \frac{\dot{B}}{B}\right)2\epsilon\dot{R} + \left(\frac{2C'}{C} - \frac{B'}{B}\right)\frac{2\epsilon A^2 R'}{B^2}\right], \tag{56}$$

$$G_{01} = q^{eff} = \frac{8\pi}{R+\varepsilon R^2}\left[\frac{2\varepsilon A'}{A}(C' + \dot{C}) + \frac{2\varepsilon C'}{B}(B' - \dot{B}) - 2\varepsilon C'^{\cdot} + kABq\right], \tag{57}$$

$$G_{11} = P_r^{eff} = \frac{1}{1+2\epsilon R}\left[P_r B^2\kappa - B^2\left(\frac{-\epsilon R^2}{2}\right) + \frac{2\epsilon B^2\ddot{R}}{A^2} - \left(\frac{2\dot{C}}{C} + \frac{\dot{A}}{A}\right)\frac{2\epsilon B^2\ddot{R}}{A^2} - 2\epsilon R'\left(\frac{2C'}{C} + \frac{A'}{A}\right)\right], \tag{58}$$

$$G_{22} = P_\perp^{eff} = \frac{1}{1+2\epsilon R}\left[P_\perp C^2\kappa - C^2\left(\frac{-\epsilon R^2}{2}\right) - \frac{2\epsilon C^2 R''}{B^2} + \frac{2\epsilon C^2\ddot{R}}{A^2} - \left(\frac{\dot{C}}{C} - \frac{\dot{B}}{B} + \frac{\dot{A}}{A}\right)\frac{2\epsilon C^2\dot{R}}{A^2} - \left(\frac{2C'}{C} + \frac{A'}{A}\right)\frac{2\epsilon C^2 R'}{B^2}\right]. \tag{59}$$

4.1 Physical significance of the $f(R)$ model

Here we examine physical importance of the function $f(R) = R + \epsilon R^2$ for stellar bodies. For this purpose, we analyze the viability of parameter ϵ associated with a compact object. Thus we consider a simple model that relies on spatial astral density (a theory same as the de Vaucoulour's statement in the exterior zone that avoids a fixed center). Hernquist and Jaffe [50,51] firstly proposed such kinds of models with central astral densities proportional to r^{-1} and r^{-2}. These models lead to a variety of energy density distributions with various central slopes described by

$$\tilde{\mu}(r) = \frac{(3-\tau)M\tilde{\alpha}}{4\pi r^\tau (r+\tilde{\alpha})^{4-\tau}}. \tag{60}$$

Here $\tilde{\alpha}$ represents a scaling radius and M shows the total mass which is in proportion to r^τ at the center. The value of τ is fixed as $[0, 3)$ whereas $\tau = 1$ and $\tau = 2$ restricts the model to Hernquist and Jaffe models, respectively. The Krori–Barua anstaz method is used to investigate the metric functions related to interior spacetime [52]. The interior spacetime is given by

$$A = e^{\tilde{a}}, \quad B = e^b, \quad C = r, \tag{61}$$

where $\tilde{a} = \tilde{B}r^2 + \tilde{C}$ and $b = \tilde{A}r^2$. To represent a realistic model for compact stellar object, we employ the Schwarzschild spacetime as exterior geometry having an asymptotically flat and static outside area. The Schwarzschild

metric is given by

$$ds^2 = \left(1-\frac{2M}{r}\right)dt^2 - \left(1-\frac{2M}{r}\right)^{-1}dr^2 - r^2\left(d\theta^2+\sin^2\theta d\phi^2\right). \quad (62)$$

We are now applying boundary conditions to both spacetimes associated with exterior and interior geometries. At the condition $r = R$, the continuity of exterior and interior line elements produces

$$g_{tt}^- = g_{tt}^+, \quad g_{rr}^- = g_{rr}^+, \quad \frac{\partial g_{tt}^-}{\partial r} = \frac{\partial g_{tt}^+}{\partial r}, \quad (63)$$

where the superscripts $(-)$ and $(+)$ represent the interior and exterior surfaces of the stellar object, respectively. Thus, Eq. (63) implies

$$\tilde{A} = -ln\left(1-\frac{2M}{r}\right)\frac{1}{R^2}, \quad \tilde{B} = \frac{M}{R^3}\left(1-\frac{2M}{r}\right)^{-1}, \quad (64)$$

$$\tilde{C} = ln\left(1-\frac{2M}{r}\right) - \frac{M}{R}\left(1-\frac{2M}{r}\right)^{-1}. \quad (65)$$

Here we examine the physical significance of the function $f(R) = R + \epsilon R^2$ for stellar systems. For this, we analyze the viability of parameter ϵ associated with a compact object. So, we consider a simple model that relies on spatial astral density (a theory same as the de Vaucoulour's statement in the exterior zone that avoids a fixed center). Hernquist and Jaffe [50,51] firstly proposed such kinds of models with central astral densities proportional to r^{-1} and r^{-2}. These models lead to a variety of energy density distributions with various central slopes described by

$$\tilde{A} = 0.010906441192\,\mathrm{km}^{-2}, \quad (66)$$

$$\tilde{B} = 0.0098809523811\,\mathrm{km}^{-2}, \quad (67)$$

$$\tilde{C} = -2.0787393571141\,\mathrm{km}^{-2}. \quad (68)$$

Substituting the values of $\tilde{A}$, $\tilde{B}$ and $\tilde{C}$ in Eqs. (56)–(59), we can explore the behaviors of energy density, radial, and tangential pressures associated to the matter distribution.

5 The purely areal evolution condition and radial velocity

Here we discuss a new definition of collapsing velocity U, previously, it is defined as the change of areal radius (C) per unit proper time. The velocity can also be defined as a variation of the infinitesimal proper radial distance between two adjacent points (δl) per unit of proper time, i.e., $D_T(\delta l)$. It has been shown that this infinitesimal rate of change is related to the shear and expansion effects, given by [36]

$$\frac{D_T(\delta l)}{\delta l} = \frac{(2\sigma+\Theta)}{3}, \quad (69)$$

which, through Eqs. (22) and (25), becomes

$$\frac{D_T(\delta l)}{\delta l} = \frac{\dot{B}}{AB}. \quad (70)$$

Using Eqs. (22), (25), (34) and (70), we obtain

$$\sigma = \frac{D_T(\delta l)}{\delta l} - \frac{D_T C}{C} = \frac{D_T(\delta l)}{\delta l} - \frac{U}{C}, \quad (71)$$

and

$$\Theta = \frac{D_T(\delta l)}{\delta l} + \frac{2D_T C}{C} = \frac{D_T(\delta l)}{\delta l} + \frac{2U}{C}. \quad (72)$$

This shows that the areal velocity U, being the variation of C (areal radius) of a layer of fluid particle, is generally different from $D_T(\delta l)$ which is the relative velocity of neighboring layers of fluid particles present within the clusters. Equation (71) shows that the collapsing stars cluster, having $U < 0$, becomes shearless if $D_T(\delta l) < 0$, i.e., the relative distance between the layers of cluster particles vanishes in such a way that it cancels out the values of U. Equation (72) describes that an expansion-free situation is possible if the areal velocity U cancels out the relative velocity $D_T(\delta l)$. So for collapsing expansion-free case, we have $U < 0$ and $D_T(\delta l) > 0$. Alternatively, for the outgoing case $(U > 0)$, expansion-free condition is possible if $D_T(\delta l) < 0$. Moreover, it has been shown that the existence of a cavity requires a purely areal evolution condition described by $D_T(\delta l) = 0$ with $U \neq 0$ [39]. Thus, to derive cavity solutions within cluster distribution, let us assume the condition $D_T(\delta l) = 0$ with $U \neq 0$. This, along with Eqs. (71) and (72), implies $\theta = -2\sigma$. Using this result in Eq. (16), we get

$$\sigma' + \frac{\sigma C'}{C} = -\frac{4\pi q^{eff} C'}{E}, \quad (73)$$

whose integration with respect to r gives

$$\sigma = \frac{\zeta(t)}{C} - \frac{4\pi}{C}\int_0^r q^{eff}\frac{CC'}{E}dr, \quad (74)$$

with $\zeta(t)$ being an integration function. It can be noticed that in the situation when all the spherical surfaces of a cluster of stars including the center $(r = 0)$ is filled with baryonic as well as non-baryonic fluids, we should imply the regularity condition $(\zeta = 0)$. As we are interested in the formation of the cavity around the center, such condition is not needed. In other case, Eq. (74) with (71) leads to

$$U = -\zeta + 4\pi\int_0^r q^{eff}\frac{CC'}{E}dr. \quad (75)$$

Hence, for non-dissipative case $(q^{eff} = 0 \Rightarrow q^M = q^D = 0)$, the purely areal evolution condition suggests $U = U(t)$. This result is certainly unsuitable with a regular symmetry center except $(U = 0)$. To have a purely areal evolution condition to be compatible with a time dependent stage $(U \neq 0)$, this yields

- The cluster has no symmetry center.
  Or
- The center is encircled by a compact spherical region of other spacetime, appropriately matched to the rest of the fluid inside the cluster.

Here we are going to reject the first case because this indicates the unusual geometry of a star cluster without a center. Furthermore, for the second case, we select Minkowski's inner vacuum spherical vacuole. It can be noticed that dissipation due to DM (q^D) might be some sort of squandering of non-baryonic particles. This type of dissipation is due to the gravitational energy of DM. Now a question arises here, can we consider a non-dissipation case in the presence of DM? The evidence of DM is based upon its gravitational effects so the dissipation due to DM gravitational effects can not be neglected easily. Hence during the evolution of the cluster of stars having DM, the non-dissipative case is very special or unusual.

Let us now assume an alternative case that entirely belongs to areal dissipative evolution ($D_T(\delta l) = 0$). If the gravitating fluid (for baryonic as well as non-baryonic parts) fills the entire spherical cluster, we get a symmetry center and there is no cavity surrounding the center. In this situation, we need to put $\zeta = 0$ such that Eq. (75) becomes

$$U = 4\pi \int_0^r q^{eff} \frac{CC'}{E} dr, \tag{76}$$

which is congruent with a regular symmetric center. For this situation, we shall consider a cavity enclosing the center in an ad hoc manner. The following subjective argument can propose this assumption. Consider an outwardly dissipative condition ($q^{eff} > 0$) which implies that all the terms inside the integral are positive such that Eqs. (72) and (76) give $\Theta > 0$, $U > 0$. Inversely, for $q^{eff} < 0$, we get $\Theta < 0$, $U < 0$. Since we are dealing with dissipation due to matter and DM so one of the sources for this dissipation is the gravitational energy. Moreover, according to Kelvin–Helmholtz evolution phase [55], when all the outgoing dissipative flux originates from the gravitational energy, we should anticipate contraction instead of expansion. In contrast, inwardly directed flux of dissipation leads to expansion. The above discussion shows that dissipation due to heat flux behaves differently from dissipation due to gravitational energy. So the outgoing dissipation due to DM ($q^D > 0$) contributes to the contraction phase of the evolution and inversely, $q^D < 0$ helps in expansion of the evolving cluster. Hence, we observe that the condition $D_T(\delta l) = 0$ (purely areal evolution phase) shows up to be particularly appropriate for describing evolution of a cluster of stars with a cavity enclosing the center [39]. Finally, using Eqs. (71) and (72) in (26), the purely areal evolution phase can be described as

$$\sigma_{\iota\omega} = -\frac{\Theta}{2}\left(\chi_\iota \chi_\omega - \frac{1}{3} h_{\iota\omega}\right). \tag{77}$$

Next, we shall explore some models for cluster of stars having purely areal evolution.

5.1 Models of cavities in clusters

In this section, we explore the general characteristics of models of clusters that satisfy the purely areal evolution case. Here we use the general concept similar to that suggested by Skripkin [35]. According to his proposal, an explosion at the center causes an overall expansion throughout the fluid, resulting in the development of a cavity around the center. But, here is the distinction that we are considering purely areal evolution $D_T(\delta l) = 0$ rather $\Theta = 0$. In this context, Eq. (70) implies $\dot{B} = 0$ ($\dot{C} \neq 0$) which gives $B = B(r)$ and we can take $B = 1$ without the loss of generality. As previously indicated, the physical importance of this sort of model comes from the fact that the condition $\dot{B} = 0$ requires the existence of a center-based cavity. For this case, the field equations become

$$8\pi\mu = \frac{A^2}{1+2\epsilon R}\left[\frac{1}{A^2}\left(\frac{\dot{C}}{C}\right)^2 - 2\frac{C''}{C} - \left(\frac{C'}{C}\right)^2 + \frac{1}{C^2}\right] - \left[2\epsilon A^2 R'' + \left(\frac{2\dot{C}}{C}\right)2\epsilon\dot{R} + \left(\frac{2C'}{C}\right)2\epsilon A^2 R'\right], \tag{78}$$

$$8\pi q = \frac{A}{1+2\epsilon R}\left(\frac{\dot{C}'}{C} - \frac{\dot{C}}{C}\frac{A'}{A}\right) - \left[\frac{2\varepsilon A'}{A}(C'+\dot{C}) + 2\varepsilon C' - 2\varepsilon \dot{C}'\right], \tag{79}$$

$$\begin{aligned} 8\pi P_r = &-\frac{1}{1+2\epsilon R}\left[2\frac{\ddot{C}}{C} - \left(2\frac{\dot{A}}{A} - \frac{\dot{C}}{C}\right)\frac{\dot{C}}{C}\right] \\ &+\left(2\frac{A'}{A} + \frac{C'}{C}\right)\frac{C'}{C} - \frac{1}{C^2} \\ &-\left(\frac{-\epsilon R^2}{2}\right) + \frac{2\epsilon\ddot{R}}{A^2} - \left(\frac{2\dot{C}}{C} + \frac{\dot{A}}{A}\right)\frac{2\epsilon\dot{R}}{A^2} \\ &-2\epsilon R'\left(\frac{2C'}{C} + \frac{A'}{A}\right)\Big], \end{aligned} \tag{80}$$

$$\begin{aligned} 8\pi P_\perp = &-\frac{1}{(1+2\epsilon R)A}\left(\frac{\ddot{C}}{C} - \frac{\dot{A}}{A}\frac{\dot{C}}{C}\right) + \frac{A''}{A} \\ &+\frac{C''}{C} + \frac{A'}{A}\frac{C'}{C} - C^2\left(\frac{-\epsilon R^2}{2}\right) \\ &-2\epsilon C^2 R'' + \frac{2\epsilon C^2\ddot{R}}{A^2} - \left(\frac{\dot{C}}{C} - \frac{\dot{A}}{A}\right)\frac{2\epsilon C^2\dot{R}}{A^2} \end{aligned}$$

$$-\left(\frac{2C'}{C}+\frac{A'}{A}\right)2\epsilon C^2R'\Big]. \tag{81}$$

Also, the non-zero parts of the Bianchi identities $T^{(eff)-\alpha\beta}_{;\beta}=0$ are given by

$$\begin{aligned}
&\frac{1}{A}\Big[\dot{\mu}+\frac{2}{1+2\epsilon R}\left\{\left(\mu A^2+P_\perp C^2\right)\kappa\right.\\
&+\left(A^2-C^2\right)\left(f-R+2\epsilon R^2\right)\\
&-2\epsilon R''\left(A^2+C^2\right)+\frac{2\epsilon A^2\dot{R}}{A^2}\left(\frac{2\dot{C}}{C}\right)\\
&+\frac{2\varepsilon C^2\ddot{R}}{A^2}-\left(\frac{\dot{C}}{C}+\frac{\dot{A}}{A}\right)\frac{2\epsilon C^2\dot{R}}{A^2}\\
&\left.+\left(\frac{2C'}{C}\right)\epsilon A^2R'-\left(\frac{2C'}{C}+\frac{A'}{A}\right)\epsilon C^2R'\right\}\frac{\dot{R}}{R}\Big]+q'\\
&+\frac{2}{1+2\epsilon R}\Big[A\kappa q+\frac{2\epsilon A'}{A}\left(C'+\dot{C}\right)+2\epsilon C'\\
&-2\varepsilon C'\cdot\Big]\frac{(AR)'}{AR}=0,
\end{aligned} \tag{82}$$

$$\begin{aligned}
&\frac{1}{A}\left[\dot{q}+\frac{2}{1+2\epsilon R}\left(A\kappa q+\frac{2\epsilon A'}{A}(C'+\dot{C})+2\epsilon C'\dot{C}-2\epsilon\right)\right]\\
&+P_r{}'+\frac{1}{2\epsilon R}\Big[(\mu A^2+P_r)\kappa+(A^2)\left(\frac{\epsilon R^2}{2}\right)\\
&-2\epsilon A^2R''+\frac{2\epsilon\ddot{R}}{A^2}+\left(\frac{2\dot{C}}{C}\right)2\epsilon\dot{R}+\left(\frac{2C'}{C}\right)2\epsilon A\dot{R}\\
&-\left(\frac{2\dot{C}}{C}+\frac{\dot{A}}{A}\right)\frac{2\epsilon\epsilon\dot{R}}{A^2}-\left(\frac{2C'}{C}+\frac{A'}{A}\right)2\epsilon R'\Big]\frac{A'}{A}\\
&+\frac{2}{1+2\epsilon R}\Big[(P_r+P_\perp C^2)\kappa+C^2)\left(\frac{\epsilon R^2}{2}\right)\\
&+\frac{2\epsilon\ddot{R}}{A^2}-\left(\frac{2\dot{C}}{C}+\frac{\dot{A}}{A}\right)\frac{2\epsilon\dot{R}}{A^2}\\
&-\left(\frac{2C'}{C}+\frac{A'}{A}\right)2\epsilon R'+2\epsilon C^2R''\\
&-\frac{2\epsilon C^2\ddot{R}}{A^2}+\left(\frac{\dot{C}}{C}+\frac{\dot{A}}{A}\right)\frac{2\epsilon C^2\dot{R}}{A^2}\\
&+\left(\frac{C'}{C}+\frac{A'}{A}\right)2\epsilon C^2R'\Big]\frac{R'}{R}=0.
\end{aligned} \tag{83}$$

In specific geodesic condition, we have $A'=0$ which implies $A=1$. At this point, the field equations (79)–(81) become

$$\begin{aligned}
8\pi\mu=&\frac{1}{1+2\epsilon R}\left[\left(\frac{\dot{C}}{C}\right)^2-2\frac{C''}{C}-\left(\frac{C'}{C}\right)^2+\frac{1}{C^2}\right]\\
&-\left[2\epsilon R''+\left(\frac{2\dot{C}}{C}\right)2\epsilon\dot{R}+\left(\frac{2C'}{C}\right)2\epsilon R'\right],
\end{aligned} \tag{84}$$

$$8\pi q=\frac{1}{1+2\epsilon R}\left(\frac{\dot{C}'}{C}-\frac{\dot{C}}{C}\right)-\left[2\varepsilon(C'+\dot{C})\right], \tag{85}$$

$$\begin{aligned}
8\pi P_r=&-\frac{1}{1+2\epsilon R}\left[2\frac{\ddot{C}}{C}+\left(\frac{\dot{C}}{C}\right)\frac{\dot{C}}{C}\right]\\
&+\left(\frac{C'}{C}\right)\frac{C'}{C}-\frac{1}{C^2}-\left(\frac{-\epsilon R^2}{2}\right)+2\epsilon\ddot{R}\\
&-\left(\frac{2\dot{C}}{C}\right)2\epsilon\ddot{R}-2\epsilon R'\left(\frac{2C'}{C}\right)\Big],
\end{aligned} \tag{86}$$

$$\begin{aligned}
8\pi P_\perp=&-\frac{1}{(1+2\epsilon R)}\left(\frac{\ddot{C}}{C}\right)+\frac{C''}{C}\\
&+\left(\frac{-\epsilon R^2}{2}\right)-2\epsilon C^2R''+2\epsilon C^2\ddot{R}\\
&-\left(\frac{\dot{C}}{C}\right)2\epsilon C^2\dot{R}-\left(\frac{2C'}{C}\right)2\epsilon C^2R'\Big].
\end{aligned} \tag{87}$$

It follows from Eq. (31) that

$$\begin{aligned}
2\pi\mu^{eff}&=\frac{m}{R^3}+(2\pi P_r{}^{eff}-2\pi P_\perp{}^{eff}),\\
2\pi(\mu+\mu^D)&=\frac{m}{R^3}(2\pi P_r+2P_\perp)+(2\pi P_r^D-2P_\perp^D).
\end{aligned} \tag{88}$$

Equation (44) implies

$$\begin{aligned}
2\pi\mu^{eff}&=(2\pi P_r{}^{eff}-4\pi P_\perp{}^{eff})-\varepsilon,\\
(\mu^m+\mu^D)&=(2\pi(P_r^M-2P_\perp^M))+(2\pi(P_r^D-2P_\perp^D))-\varepsilon.
\end{aligned} \tag{89}$$

Thus, Eqs. (88) and (89) under conformally flat ($\varepsilon=0$), geodesic and isotropic case ($P_r^{eff}=P_\perp^{eff}=P^{eff}$) provide

$$\frac{m}{C^3}+4\pi P^{eff}=0. \tag{90}$$

This along with Eq. (51) implies that the respective model satisfies Dramois junction conditions only for its absorbing dissipative energy behavior, i.e., $q^{eff}<0$ otherwise, we get $M=0,\quad m<0$. Furthermore, the condition $q^{eff}<0$ implies two possibilities either $q<-q^D$ or $q^D<-q$.

5.2 Model consistent with Darmois conditions

Now we consider some simplified analytical models that are not based upon thin shells either $\Sigma^{(e)}$ or $\Sigma^{(i)}$, but are consistent with Darmois conditions. In this context, the non-dissipative models are found to be the simplest ones. Taking $q^{eff}=0$ along with Eq. (79), integration gives

$$A=\frac{\dot{C}}{h_1}, \tag{91}$$

where $h_1(t)$ is an integration function of t. Without loss of generality, after re-parameterizing t, we can assume

$$h_1=\dot{C}_{\Sigma^{(i)}}, \tag{92}$$

with

$$A_{\Sigma^{(i)}}=1. \tag{93}$$

It can be noticed from Eqs. (34) and (91) that the velocity U becomes

$$U = h_1 = \dot{C}_{\Sigma^{(i)}}, \tag{94}$$

which remains same for all particles present in the cluster fluid. This point has already been discussed with Eq. (75) in the previous section. Substituting Eq. (91) into (79), (80) and (81) and using Eqs. (32), (91) and (92), we get

$$8\pi\mu^{eff} = -\frac{1}{C^2}\left(2CC''^2 + C'^2 - \dot{C}^2_{\Sigma^{(i)}} - 1\right), \tag{95}$$

$$8\pi P_r^{eff} = \left[\frac{1}{C^2\dot{C}}D_T\left[\frac{1}{C^2\dot{C}}D_T\left[C(C')^2 - \dot{C}^2_{\Sigma^{(i)}} - 1\right]\right]\right], \tag{96}$$

$$8\pi P_\perp^{eff} = \frac{1}{2C\dot{R}_{\Sigma^{(i)}}}D_T\left(2CC'' + C'^2 - \dot{C}^2{}_{\Sigma^{(i)}} - 1\right). \tag{97}$$

From Eqs. (96) and (97), it can be observed that

$${P_\perp}^{eff} = -\frac{D_T(\mu^{eff}C^2)}{2C\dot{C}_{\Sigma^{(i)}}}. \tag{98}$$

Computing function of mass (31) with (91) and $B = 1$, we have

$$m = -\frac{C}{2}(C'^2 - \dot{C}^2{}_{\Sigma^{(i)}} - 1), \tag{99}$$

which turns Eq. (96) into

$$4\pi P_r^{eff} = -\frac{\dot{m}}{C^2\ddot{C}}. \tag{100}$$

Moreover, this model automatically satisfies the junction conditions $P_r^{(eff)\Sigma^{(e)}}_{=}0$, $P_r^{(eff)\Sigma^{(i)}}_{=}0$ with $m^{\Sigma^{(e)}}_{=}M = constant$ and $m^{\Sigma^{(i)}}_{=}0$. Using Eq. (91) in (43), we find

$$\epsilon = \frac{C}{4\dot{C}_{\Sigma^{(i)}}}D_T\left[\frac{1}{C^2}(2CC'' - C'^2 + \dot{C}^2{}_{\Sigma^{(i)}}) + 1\right]. \tag{101}$$

We shall now explore some specific cases.

5.2.1 Conformally flat case

If the spacetime among $r = r_{\Sigma^{(e)}}$ and $r = r_{\Sigma^{(i)}}$ is conformally flat, i.e., $\epsilon = 0$, then Eq. (101) gives

$$2CC'' + C'^2 - W_1C^2 + \dot{C}^2{}_{\Sigma^{(i)}} + 1 = 0, \tag{102}$$

where W_1 is an arbitrary function of r. After integration, we get

$$C'^2 = C\left(\int W_1 dC + h_2\right) + \dot{C}^2_{\Sigma^{(i)}} + 1. \tag{103}$$

Here $h_2(t)$ is an integration function of t. A comparison of Eqs. (99) and (103) gives

$$m = -\frac{C^2}{2}\left(\int W_1 dC + h_2\right), \tag{104}$$

such that h_2 can be obtained from the junction condition (52) given by

$$h_2\Sigma^{(i)}_{=} - \int W_1 dC. \tag{105}$$

Consequently, this sort of models are described through a single function $W_1(r)$ whose selection depends upon the satisfaction of the remaining Darmois conditions. Furthermore, the evolution is shear-free for isotropic non-dissipative spherically symmetric conformally flat spacetimes. But this is not applicable in anisotropic case. Thus, the models examined here are necessarily considered anisotropic.

5.2.2 Tangential pressureless case

Considering $P_\perp^{eff} = 0$, integration of Eq. (98) yields

$$\mu^{eff} = \frac{W_2}{C_2}, \tag{106}$$

where $W_2(r)$ is a function of r. Using Eq. (106) into (96), we have

$$2CC'' + C'^2 + 8\pi W_2 - \dot{C}^2{}_{\Sigma^{(i)}} - 1 = 0. \tag{107}$$

Also, Eq. (99) implies

$$m' = 4\pi W_2 C'. \tag{108}$$

In order to get viable models, we need to consider a particular type of energy density or mass function. For instance, let us consider

$$W_2 = c_1 = constant > 0. \tag{109}$$

In this way, Eqs. (37) and (106) imply

$$m = 4\pi c_1(C - C_{\Sigma^{(i)}}), \tag{110}$$

$$M = 4\pi c_1(C_{\Sigma^{(e)}} - C_{\Sigma^{(i)}}), \tag{111}$$

$$\dot{C}_{\Sigma^{(e)}} = A_{\Sigma^{(i)}} = A_{\Sigma^{(e)}} = 1. \tag{112}$$

Using Eqs. (100), (106) and (110), we get

$$P_r = \mu^{eff}\left(\frac{\dot{C}_{\Sigma^{(e)}}}{\dot{C}} - 1\right). \tag{113}$$

Substituting Eq. (110) into (99), we have

$$CC'^2 = \iota(t)C + \omega(t), \tag{114}$$

where

$$\iota(t) = \dot{C}^2{}_{\Sigma^{(i)}} + 1 - 8\pi c_1, \quad \omega(t) = 8\pi c_1 C_{\Sigma^{(i)}}, \tag{115}$$

whose integration gives

$$[\iota C(\iota C + \omega)]^{\frac{1}{2}} - \omega ln[(\iota R)^{\frac{1}{2}} + \iota C + \omega)]^{\frac{1}{2}}] = \iota^{\frac{2}{3}}[r - r_0]. \tag{116}$$

Here $r_0(t)$ is an integration function of t. Assessing Eq. (116) on $\Sigma^{(i)}$, we get

$$[\iota(\dot{C}_{\Sigma^{(i)}}+1)]^{\frac{1}{2}}-8\pi c_1 ln[\iota^{\frac{1}{2}}+(\dot{C}_{\Sigma^{(i)}}+1)^{\frac{1}{2}}] -4\pi c_1 lnC]C\Sigma_{=}^{(i)}\iota^{\frac{3}{2}}(r-r_0). \quad (117)$$

This shows the $1st$ order nonlinear equation for $C_{\Sigma^{(i)}}$ that can be determined for every $r_0(t)$ function. The result of this integration, combined with Eq. (116), provides the absolute information required to get r and t dependency for all metric and physical variables. It can be found that energy density within the fluid distribution remains positive and regular. Additionally, the condition $r_0(t)$ with $0<\frac{\dot{C}_{\Sigma^{(i)}}}{C}-1\leq 1$ guarantees the presence of positive pressure which is smaller than the energy density.

6 Physical conditions for stellar object

The densities and gravitational fields of the whole star cluster are different than its component star. Sometimes it becomes complex to explore the entire density and gravitational effects of the cluster of stars in strong field regimes. So for the sake of convenience and to check the physical significance of the obtained cavity model, we choose a binary star $4U182030$ as a test star from the component of compact stars cluster and check its physical features under the influences of DM. In this way, we may suggest the mutual relation between a compact star and DM in cluster of stars or galaxies. The physical viability of a compact star depends on the following conditions to be satisfied throughout the configuration:

- The metric potentials $A(r)$, $B(r)$ and the matter components μ, P_r, $P_\perp$ must be well defined at the center as well as regular within star.
- The positivity of energy density, i.e., $\mu\geq 0$ is required throughout the stellar object interior. Being positive at the center, it should be monotonically decreasing to the boundary inside the star, mathematically $\frac{d\mu}{dr}\leq 0$.
- The radial and the tangential pressures should be positive, i.e., $P_r\geq 0$, $P_\perp\geq 0$, whereas their gradient must be negative inside the stellar object configuration, i.e., $\frac{dP_r}{dr}\leq 0$ and $\frac{dP_\perp}{dr}\leq 0$. At the boundary, the radial pressure must vanish while the tangential pressure may not be zero.
- For an anisotropic fluid distribution, fulfillment of the following inequalities for either one of the energy conditions inside the configuration is required:
  1. Weak energy condition (WEC): $\mu>0;\ \mu+P_r>0$.
  2. Null energy condition (NEC): $\mu+P_r>0$.
  3. Strong energy condition (SEC): $\mu+P_r\geq 0;\ \mu+P_\perp\geq 0;\ \mu-P_r+2P_\perp$.
  4. Dominant energy conditions (DEC): $\mu\geq P_r;\ \mu\geq P_\perp$.
- The causality condition must be satisfied for physical viability of the model, i.e., the velocity of sound should be smaller than 1 in the stellar object interior. Mathematically, $0\leq V_r\leq 1$ and $0\leq V_\perp\leq 1$, where $V_r=\frac{dP_r}{d\mu}$ and $V_\perp=\frac{dP_\perp}{d\mu}$ represent the radial and transverse velocity of sound, respectively.
- The smooth matching of the interior and exterior metric functions at the boundary is also required.
- The adiabatic index Γ must be greater than $\frac{4}{3}$ for the stability of stellar object configuration.

6.1 Physical analysis with observational data of $4U1820-30$

Here, we discuss physical interpretation of the solutions obtained for cavity model. For physical compatibility of stellar model, we combine our calculations with the data obtained for the pulsar $4U1820-30$ [53,54].

6.1.1 Metric potentials

Firstly, we examine the physical viability of the model by using Eqs. (61), (66)–(68) and explore the physical behavior of gravitational potentials $A(r)$ and $B(r)$ graphically as shown in Fig. 1. It is observed that this model has finite values of $A(r)=e^{\tilde{B}r^2+\tilde{C}}$, $B(r)=e^{\tilde{A}r^2}$ at the center ($r=0$) of the star. One can also find that $A'(r=0)=0$, $B'(r=0)=0$ which depict the regularity of metric potentials at the center and also show that the metric is well-behaved throughout the interior of star. This implies fulfillment of the requirement for realistic star.

6.1.2 Energy density, pressures and their gradient

For the sake of physical analysis in $f(R)$ gravity, let us begin with the main components of matter distribution, i.e., energy density and pressures (radial and tangential). To incorporate DM effects, we take the Starobinsky model $f(R)=R+\epsilon R^2$. We have plotted graphical results in $3D$ with effects of DM for anisotropic sphere in $f(R)$ gravity by varying radial component r as well as parameter ϵ (DM parameter). In this way, we find their role in the emergence of various physical factors. To provide a comparison between the stellar object model in $f(R)$ and GR, we use data of binary pulsar $4U1820-30$. Moreover, the $2D$ illustration provides the corresponding results in GR for $\epsilon=0$.

First of all, we analyze the behavior of energy density graphically corresponding to DM ($\epsilon\neq 0$) as well as baryonic matter (in GR limits $\epsilon=0$). The behavior of matter density μ with DM effects as a function of r and ϵ is shown in

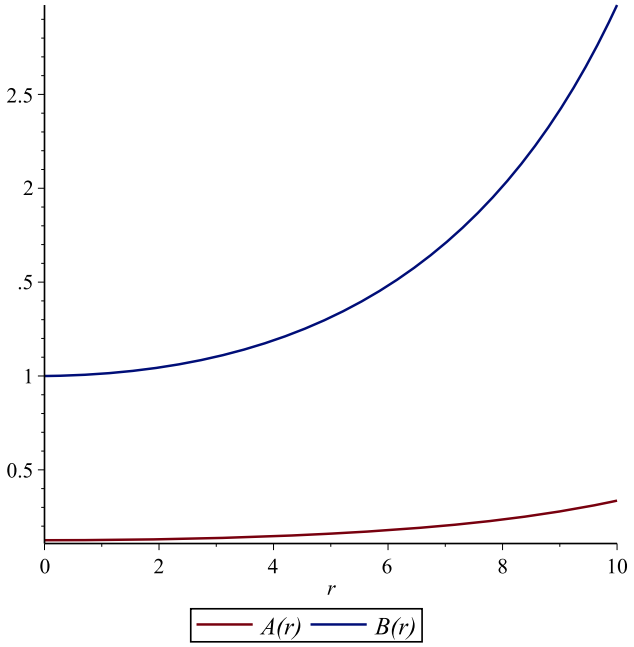

Fig. 1 Behavior of the metric potentials $A(r)$ and $B(r)$ versus r

Fig. 2 (upper panel). It can be seen that the energy density remains positive throughout the star's interior and decreases monotonically towards the boundary inside the stellar object interior but does not vanish at the boundary as ϵ increases.

The pressures under the influence of DM in the radial and tangential directions are also shown in Fig. 2 (middle and lower panels, respectively). It is noticed that the radial and the tangential pressures remain positive, i.e., $P_r \geq 0$, $P_\perp \geq 0$ throughout the cluster. For increasing values of ϵ, the radial pressure associated with DM rise to the maximum value at the center but vanishes at the boundary for all choices of ϵ (middle panel). Furthermore, the behavior of matter tangential pressure is also shown in Fig. 2 (lower panel). The tangential pressure decreases throughout the star but at the center, its value reaches a maximum as the value of ϵ increases. Thus, the pressures for both cases remain decreasing in the radial direction while the radial pressure disappears at the boundary as it should be.

We also present our results with $\epsilon = 0$ for energy density and pressures in GR limits (Fig. 3). The resultant illustration in $2D$ represents the positivity of all matter components throughout the cluster. All the three matter components remain positive throughout the interior and tend to decrease towards the boundary, whereas the tangential pressure vanishes at the boundary. Also, they attain maximum value at the center but not more than the values with DM effects $\epsilon \neq 0$. It is noticed from the above analysis that for the increasing values of ϵ, the energy density and pressure components of DM become dominant in contrast to the matter-energy density and pressures. Thus, the results in presence of DM are more consistent with observations on a cluster of stars like

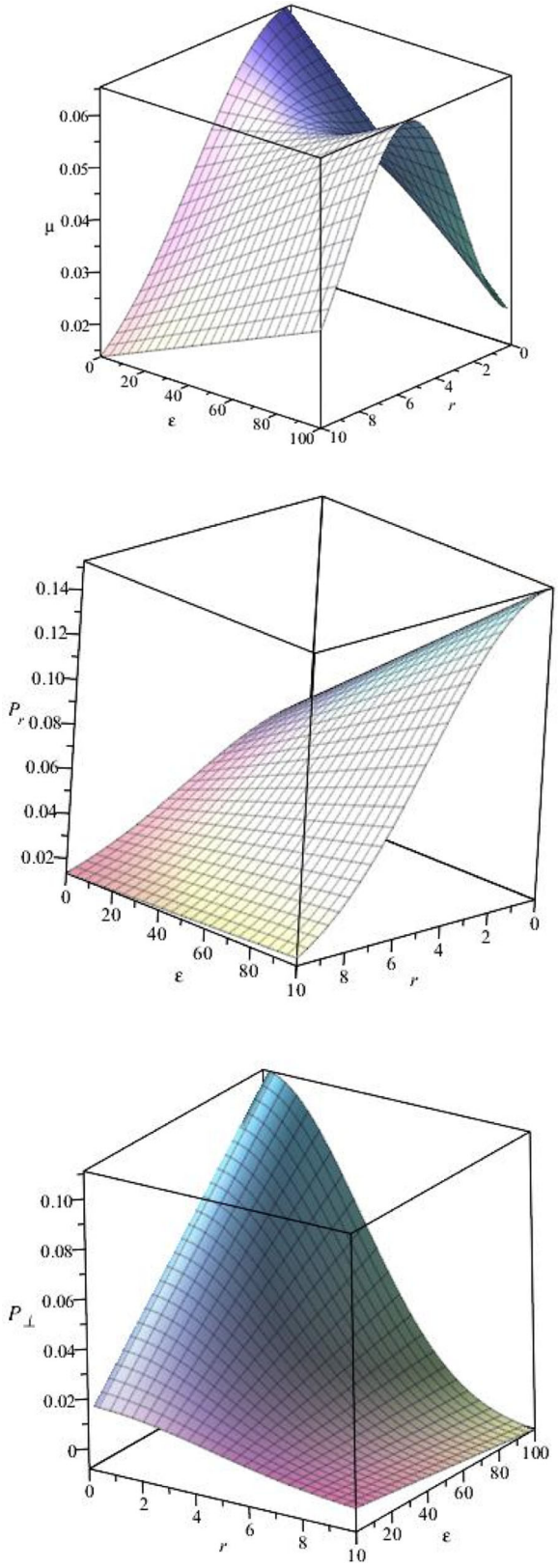

Fig. 2 Behavior of energy density, radial and tangential pressure with DM in $f(R)$

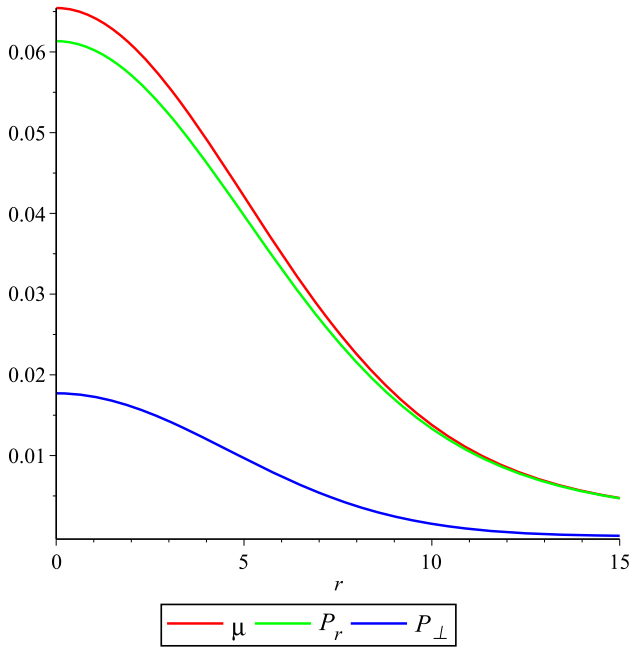

Fig. 3 Behavior of energy density, radial and tangential pressure without DM

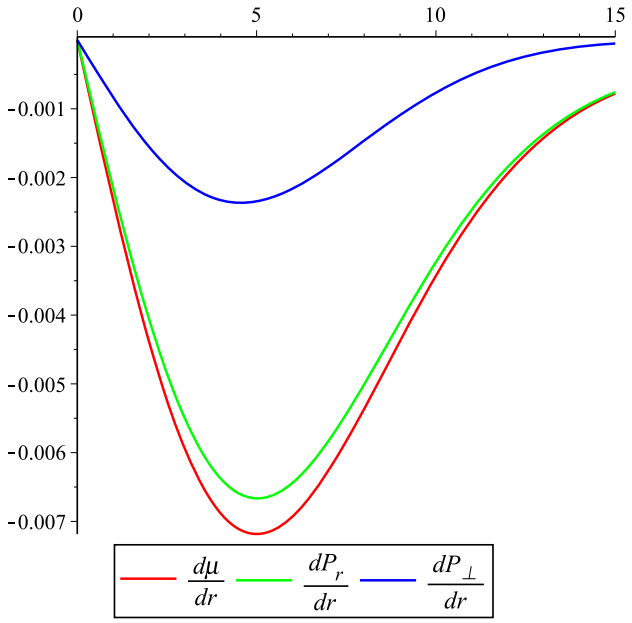

Fig. 4 Behavior of gradient of energy density, radial and tangential pressure without DM

Table 1 Gradients of energy density, radial and tangential pressure with $\epsilon = 100$

r	$\frac{d\mu}{dr}$	$\frac{dP_r}{dr}$	$\frac{dP_\perp}{dr}$
0.1	−0.1802510975	-2.6069049×10^8	−25.14206024
2	−0.1402021472	−0.2855379697	−0.5892772307
9.8	−0.5445930614	−0.003436029882	−0.8503533168

galaxy rotational curves, according to which, at the center of the cluster the density and pressure become enormous [56].

For physical viability of our cavity model, the energy density and pressure gradients should also be negative. Here we show the results for gradients in tabular form with DM effects. Table 1 shows that $\frac{d\mu}{dr} \leq 0$, $\frac{dP_r}{dr} \leq 0$ and $\frac{dP_\perp}{dr} \leq 0$ within the cavity by taking $\epsilon = 100$ and different choices of radii.

The result for energy density and pressure gradients with $\epsilon = 0$ is given in Fig. 4 which shows consistency of our results with GR, i.e., negativity of gradients within the cluster.

6.1.3 Energy conditions

We also analyze the viability of the stellar object model by energy conditions to be satisfied by the matter components of DM. It is mentioned here that for WEC, the energy density is always positive, i.e., $\mu \geq 0$ throughout the interior of a cluster as already discussed, thus we need to find the behavior of remaining energy conditions for DM. The values of energy conditions for DM with various choices of r and $\epsilon = 100$ are shown in Table 2.

For DM, it is observed that WEC, NEC and SEC are satisfied in the presence of DM. Moreover, DEC is violated at the center, whereas $\mu - P_r \geq 0$ and $\mu - P_\perp \geq 0$ for all other choices of r in the interior of the star. We have plotted the behavior of energy conditions for the matter case ($\epsilon = 0$) graphically as shown in Fig. 5. We find that all the energy conditions are satisfied throughout the star's interior in GR limits.

6.1.4 Velocity of sound

For the physical acceptability of the respective model for star, we examine causality conditions to be satisfied within the interior. The radial and transverse velocities are defined by

$$V_r = \frac{dP_r}{d\mu}, \tag{118}$$

$$V_\perp = \frac{dP_\perp}{d\mu}. \tag{119}$$

We provide the behavior of radial and transverse velocities versus r and $\epsilon = 100$ in Table 3.

It can be observed, from the table, that in the presence of DM we have $0 \leq V_r \leq 1$ and $0 \leq V_\perp \leq 1$ at the boundary. This shows that the DM affects the propagation of the speed of sound. For matter case, we also perform a graphical analysis and observe the fulfillment of causality condition, i.e., $0 \leq V_r \leq 1$ and $0 \leq V_\perp \leq 1$ (Fig. 6). It is mentioned

Table 2 Energy conditions with DM

r	$\mu + P_r$	$\mu + P_\perp$	$\mu - P_r + 2P_\perp$	$\mu - P_r$	$\mu - P_\perp$
0.005	63695.82429	0.1322992	997.657158	332.3902	−665.135
7	0.1103568897	0.06443724160	0.01851759348	0.00776	0.0537
9.8	0.05236487184	0.02622272593	0.0000805800146	0.015740	0.04188

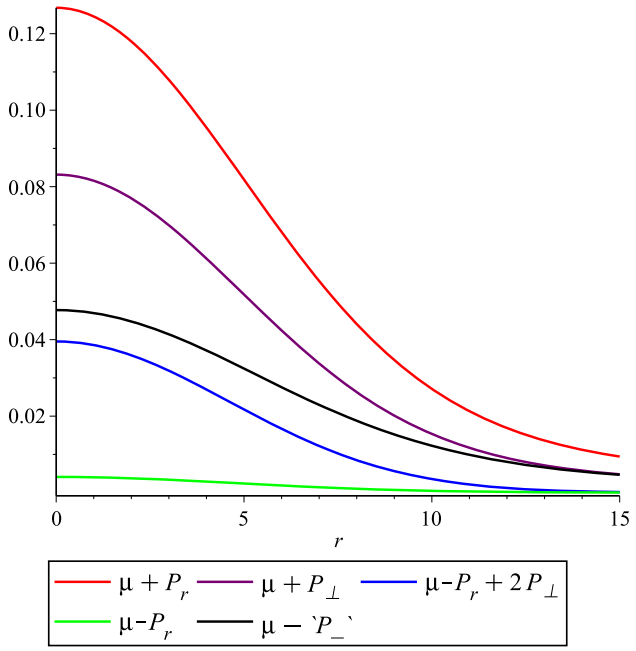

Fig. 5 Energy conditions for $\epsilon = 0$

Table 3 Sound velocities with DM

r	V_r	$V_\perp$
0.005	1.999999414	−0.9999998211
7	2.220043251	1.315799558
9.8	0.8957328381	0.1401016905

here that the requirement of smooth matching of the interior and exterior metric functions at the boundary is already performed in Sect. 5.2.

6.1.5 Adiabatic index

The adiabatic index is related to the stability of a relativistic anisotropic stellar object configuration. Mathematically, it is defined as

$$\Gamma = \frac{\mu + P}{P}\frac{dP}{d\mu}. \tag{120}$$

For physical viability of stellar object model, Γ must be greater than $\frac{4}{3}$ leading to stable configurations. We analyze

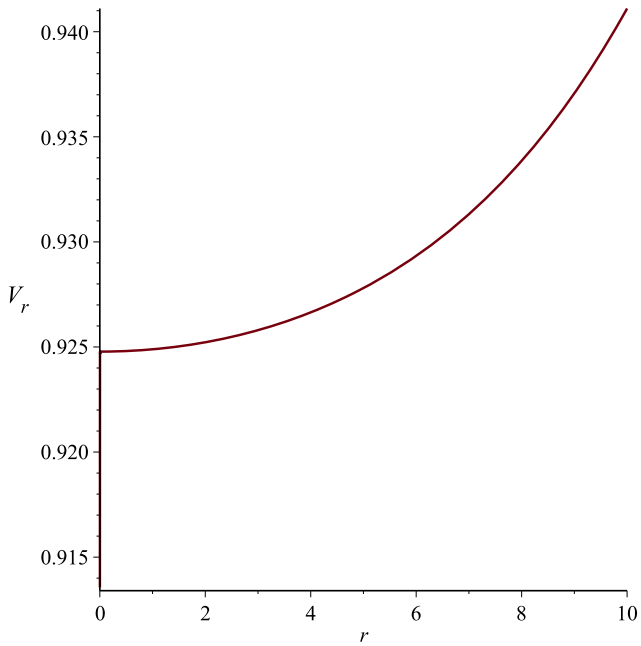

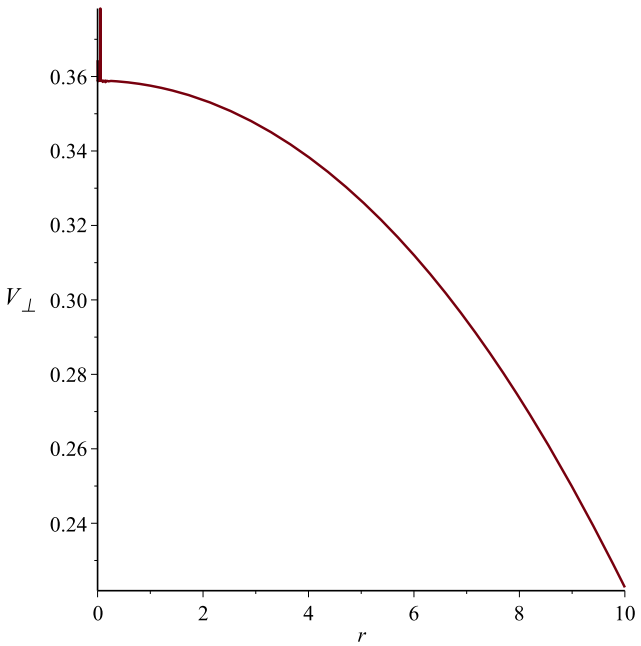

Fig. 6 Radial and transverse velocities versus r in GR

Table 4 Adiabatic index with DM for $\epsilon = 100$

r	Γ for $\epsilon = 10$	Γ for $\epsilon = 100$
0.005	2.999223808	3.000165896
7	2.233458361	4.776060977
9.8	1.993202103	2.561380308

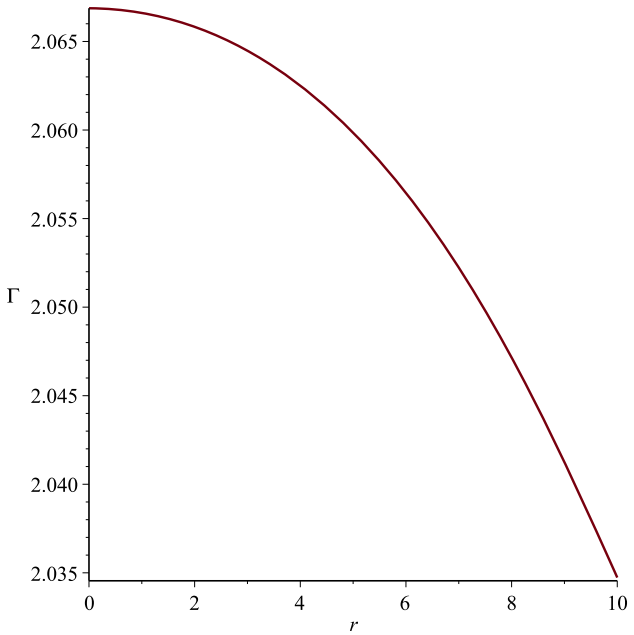

Fig. 7 Adiabatic index versus r without DM

the behavior of Γ with DM effects as given in Table 4 which appears consistent with the required condition.

We plot the behavior of adiabatic index for ordinary matter as shown in Fig. 7 which also depicts $\Gamma > \frac{4}{3}$.

7 Conclusion

The study of evolving cluster of stars has been of great interest for the description of phenomena like DM, voids and galactic structures. It is believed that the cavity model described by purely evolution conditions might be used as a void predecessor. Voids have made a major contribution to the scientific understanding of the cosmos. In this paper, we have investigated the evolution of the cavity within a spherically symmetric compact stars clusters. Generally, voids are neither spherical nor empty (according to redshift and simultaneously observations), however for sake of simplicity, they are shown as a vacuum spherical cavity surrounded by a fluid. We have resembled the cluster by a self-gravitating fluid where the collection of fluid particles represents a collection of stars (baryonic matter) and DM particles (non-baryonic matter). To accommodate DM's contribution in the discussion, we have adopted the idea of high curvature gravity ($f(R)$ gravity). We have investigated the impact of non-baryonic matter on the evolution of cavities within the cluster by using Starobinsky model, $f(R) = R + \epsilon R^2$. Specifically, we have analyzed the significance of the Starobinsky model for the evolving cluster. For this purpose, we have explored the behaviors of matter and DM by using data associated with star $4U\,1820-30$. It is found that the role of DM is dominant in contrast to the baryonic matter.

We have applied purely areal evolution condition to discuss the presence of cavity around the center. All dynamic equations under this condition have been derived and various models have been discussed. The obtained models are associated with various features like expansion-free, geodesic and conformally flat conditions. These models satisfy Darmois junction conditions for both hypersurfecs $\Sigma^{(i)}$ and $\Sigma^{(e)}$ in the presence of DM and normal matter. We have found that the evolution of cavity in cluster of stars is deeply controlled by the effects of DM. Finally, we perform the physical analysis of the obtained cavity models by relating them with the data of star $4U\,1820-30$ and investigated the physical viability of the star configuration. In this context, we have analyzed behavior of various physical factors within the cavity and compared our results with that in GR. It is found that the contribution of density and pressure becomes maximum at the center which gradually tends to decrease towards the boundary whereas their gradients remain negative throughout the stellar object interior. It is worth mentioning that our results with DM are well consistent with GR except the case for tangential pressure. For DM, the DEC is violated at the center of stellar object cluster as compared to the conditions in GR. Moreover, our stellar object cluster model is stable with $\Gamma > \frac{4}{3}$ in the presence of DM. We conclude that the inclusion of DM significantly controls the evolutionary mechanism of cavity in cluster of stars.

Data Availability Statement This manuscript has no associated data or the data will not be deposited. [Authors' comment: There is no observational data related to this article.]

Funded by SCOAP[3]. SCOAP[3] supports the goals of the International Year of Basic Sciences for Sustainable Development.

References

1. Planck collaboration, P.A.R. Ade et al., Planck 2013 Results. I. Overview of products and scientific results. Astron. Astrophys. **571**, A1 (2014)
2. J.D. Barrow, A.C. Ottewill, J. Phys. A Math. Gen. **16**(12), 2757 (1983)
3. S. Nojiri, O. Obregon, S.D. Odintsov, K.E. Osetrin, Phys. Lett. B **458**(1), 19–28 (1999)
4. S.I. Nojiri, S.D. Odintsov, IJGMMP **4**(01), 115–145 (2007)
5. A. De Felice, S. Tsujikawa, Living Rev. Relativ. **13**(1), 1–161 (2010)
6. S.I. Nojiri, S.D. Odintsov, Phys. Rep. **505**(2–4), 59–144 (2011)
7. S. Capozziello, M. De Laurentis, Phys. Rep. **509**(4–5), 167–321 (2011)
8. S. Nojiri, S.D. Odintsov, V.K. Oikonomou, Phys. Rep. **692**, 1–104 (2017)
9. G.C. Boehmer et al., Astropart. Phys. **29**, 386 (2008)
10. S. Capazziello, M.F. De- Laurentis, Ann. Phys. **524**, 545 (2012)
11. S. Capozzilleo, Int. Mod. Phys. **D11**, 483 (2002)
12. S. Nojiri, S.D. Odintsov, Phys. Rep. **505**, 59 (2011)
13. S. Capozziello et al., Phys. Rev. D **83**, 064004 (2011)
14. A.A. Starobinsky, Phys. Lett. B **91**, 99 (1980)
15. S. Gottlöber, V. Müller, A.A. Satrobinsky, Phys. Rev. D **43**, 2510 (1991)
16. J.A.R. Cembranos et al., J. Cosmol. Astropart. Phys. **4**, 021 (2012)
17. R. Florent, New Astron. Rev. **81**, 1–38 (2018)
18. E. Pcontal, T. Buchert, P. Di Stefano, Y. Copin, K. freese, E.A.S. Ser. **36**, 112–126 (2009)
19. H. Baumgardt, J. Makino, Mon. Not. R. Astron. Soc. **340**(1), 227–246 (2003)
20. A. Praagman, J. Hurley, C. Power, New Astron. **15**(1), 46–51 (2010)
21. J.H. Oort, Astron. Inst. Neth. **6**, 249 (1932)
22. J.H. Oort, Astron. Inst. Neth. **494**, 45 (1960)
23. W.H. Zwicky, Phys. Acta. **6**, 110 (1933)
24. M. Sharif, R. Manzoor, Phys. Rev. D **91**, 024018 (2015)
25. S. Rani et al., Eur. Phys. J. C **78**, 1 (2016)
26. A. Jawad et al., Phys. Dark Univ. **21**, 70 (2018)
27. Z. Yousaf, Eur. Phys. J. Plus **134**, 245 (2019)
28. R. Manzoor et al., Eur. Phys. J. C **79**, 831 (2019)
29. R. Manzoor, M. Adeel, M. Saeed, IJMPD **29**, 2050036 (2020)
30. R. Van de Weygaert, E. Platen, Int. J. Mod. Phys. Conf. Ser. **1**, 41–66 (2011)
31. D.L. Wiltshire, Dark matter in astroparticle and particle physics, pp. 565–596 (2008)
32. F. Hoyle, M.S. Vogeley, Astrophys. J. **607**(2), 751 (2004)
33. A.V. Tikhonov, I.D. Karachentsev, Astrophys. J. **653**(2), 969 (2006)
34. L. Rudnick, S. Brown, L.R. Williams, Astrophys. J. **671**(1), 40 (2007)
35. V.A. Skripkin, Sov. Phys. Dokl. **135**, 1183 (1960)
36. L. Herrera, N.O. Santos, A. Wang, Phys. Rev. D **78**, 084026 (2008)
37. L. Herrera, G. Le Denmat, N.O. Santos, Phys. Rev. D **79**, 087505 (2009)
38. G. Darmois, Mèmorial des Sciences Mathèmatiques, Fasc. 25 (Gauthier-Villars, Paris, 1927)
39. L. Herrera, G. Le Denmat, N.O. Santos, Class. Quantum Gravity **27**, 135017 (2010)
40. O.H. Billett, D.A. Hunter, B.G. Elmegreen, Astron. J. **123**, 1454 (2002)
41. M. Sharif, M.Z.U.H. Bhatti, Astrophys. Space Sci. **352**(2), 883 (2014)
42. Z. Yousaf, Eur. Phys. J. C **76**(5), 1 (2016)
43. M. Sharif, S. Mumtaz, Gen. Relativ. Gravit. **48**, 92 (2016)
44. M. Sharif, S. Mumtaz, Mon. Not. R. Astron. Soc. **471**, 1215 (2017)
45. M. Sharif, S. Mumtaz, Eur. Phys. J. Plus **132**, 436 (2017)
46. R. Maartens, arXiv:astro-ph/9609119
47. L. Herrera, A. Di Prisco, J. Ospino, Gen. Relativ. Gravit. **42**, 1585 (2010)
48. C. Misner, D.D. Sharp, Phys. Rev. B **571**, 136 (1964)
49. M. Cahill, G.J. McVittie, Math. Phys. **11**, 1382 (1970)
50. L. Hernquist, Astro Phys. J. **356**, 359 (1990)
51. W. Jaffe, MNRAS **202**, 995 (1983)
52. K.D. Krori, J. Barua, J. Phys. A Math. Gen. **8**, 508 (1975)
53. W. Zhang et al., Astro Phys. J. **L500**, 171 (1998)
54. T. Guver et al., Astro Phys. J. **719**, 1807 (2010)
55. R. Kippenhahn, A. Weigert, *Stellar structure and evolution* (Springer, Berlin, 1990)
56. S. Das, F. Rahaman, L. Baskey, Eur. Phys. J. C **79**, 853 (2019)